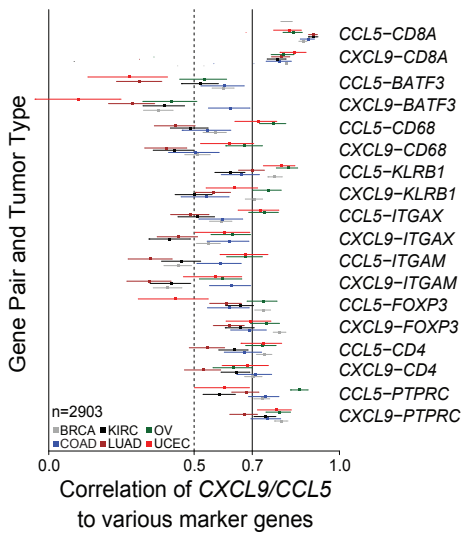


## Figure S1 related to Figure 1

### **CD8<sup>+</sup> T-cell infiltration in tumors correlates with *CXCL9* and *CCL5* chemokine expression.**

(A) Pearson correlation plots of *CD8A* with *CD3E* mRNA levels in ovarian cancer in microarray gene expression datasets. (B) Pearson correlation plots of *CD8A* and *CD3E* or *CD3D* mRNA levels in microarray gene data from different tumor types. (C) Correlation analyses of *CD8A* expression with that of genes of *CCL* and *CXCL* chemokines in the TCGA dataset. Average  $r$  (square) in a subset of 6 tumor types was plotted with 95% confidence intervals (CI) (lines) truncated on the left (n=2903). (D-E) Meta-analytical estimation of the correlation between expressions of *CD8A* with *CCL5* (D) or with *CXCL9* (E) for 17 tumor types (n=7777). Estimates (squares) are drawn in proportion to the standard errors. Lines indicate 95% CIs and diamond shows the pooled effect size at its center. TCGA abbreviations: BLCA (Bladder Urothelial Carcinoma), BRCA (Breast invasive carcinoma), CESC (Cervical squamous cell carcinoma and endocervical adenocarcinoma), COAD (Colon adenocarcinoma), HNSC (Head and Neck squamous cell carcinoma), KIRC (Kidney renal clear cell carcinoma), KIRP (Kidney renal papillary cell carcinoma), LGG (Brain Lower Grade Glioma), LIHC (Liver hepatocellular carcinoma), LUAD (Lung adenocarcinoma), LUSC (Lung squamous cell carcinoma), OV (Ovarian serous cystadenocarcinoma), PRAD (Prostate adenocarcinoma), SARC (Sarcoma), SKCM (Skin Cutaneous Melanoma), STAD (Stomach adenocarcinoma), THCA (Thyroid carcinoma). (F) Pearson correlation plots of *CD3E*, *CD247*, *CXCL9* and *CCL5* with *CD8A* quantified by qRT-PCR in an independent set of 57 stage III ovarian cancer specimens. Correlation coefficients ( $r$ ) and  $p$  values are as displayed.

A



B

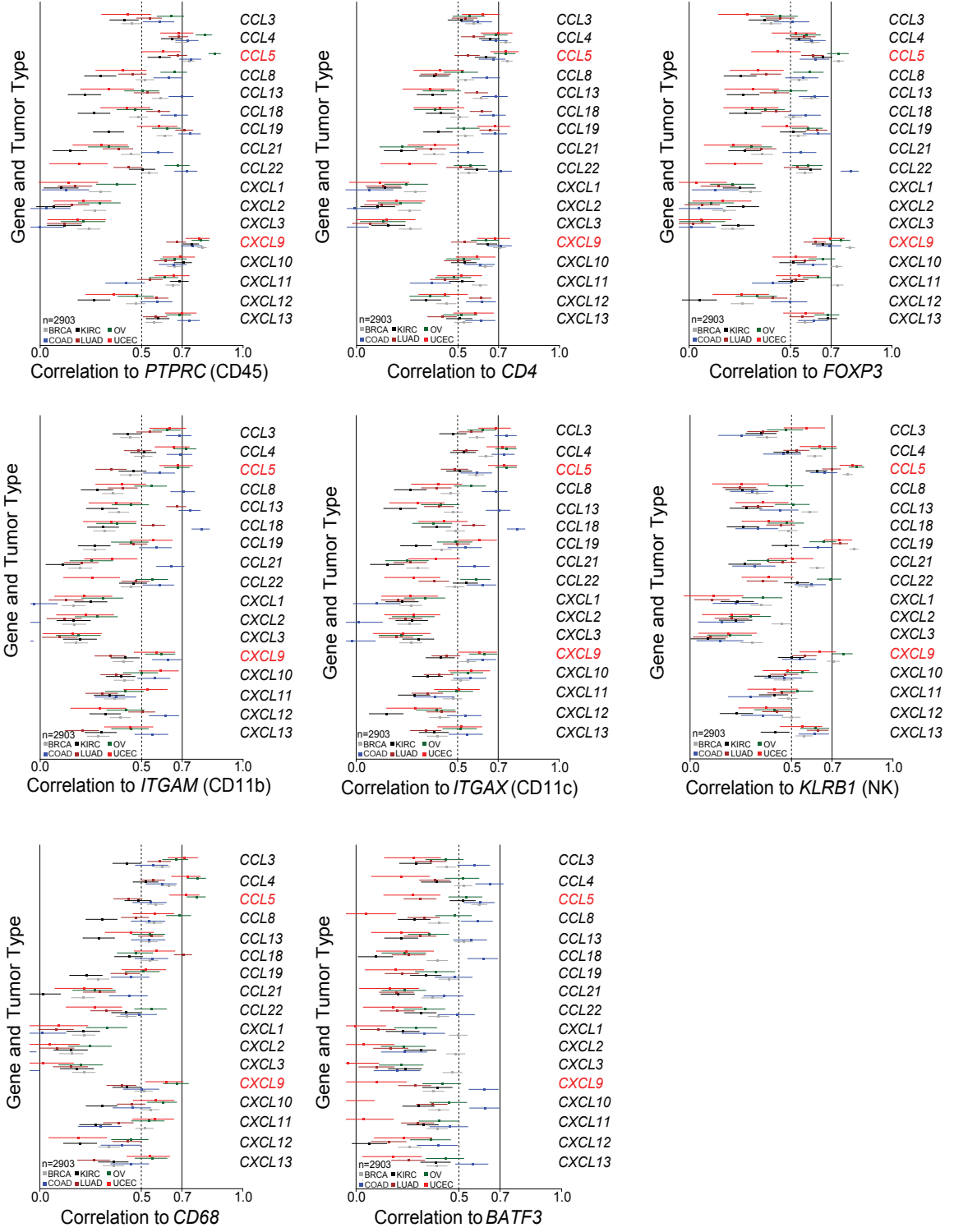


**Figure S2 related to Figure 1**

**Correlation of *CXCL9* and *CCL5* chemokine expression with immune cell subset genes in solid tumors**

**(A)** Correlation analyses of *CD8A*, *BATF3*, *CD68*, *KLRB1*, *ITGAX*, *ITGAM*, *FOXP3*, *CD4*, *PTPRC* and genes of the *CCL5* and *CXCL9* chemokines in the TCGA dataset. Average  $r$  (square) in a subset of 6 tumor types was plotted with 95% confidence CI (lines) truncated on the left (n=2903). **(B)** Correlation analyses of *BATF3*, *CD68*, *KLRB1*, *ITGAX*, *ITGAM*, *FOXP3*, *CD4*, *PTPRC* with CCL and CXCL chemokine genes in the same dataset. Average  $r$  (square) in a subset of 6 tumor types was plotted with 95%CI (lines) truncated on the left (n=2903).



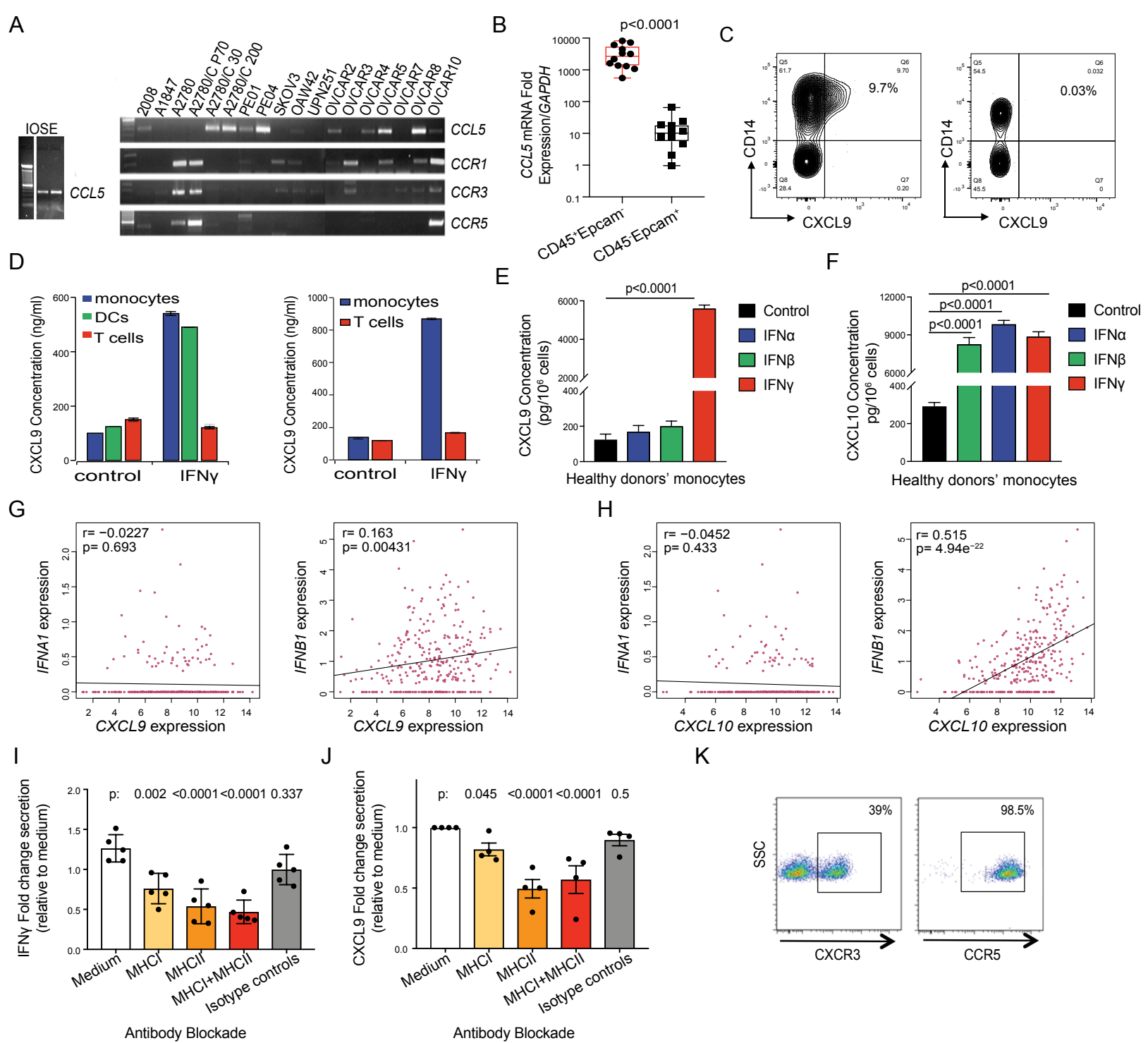


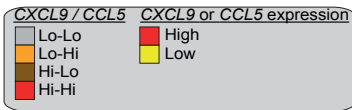
## Figure S3 related to Figures 2, 3 and 4

### Characterization of CCL5, CXCL9 and CXCL10 in ovarian cancer

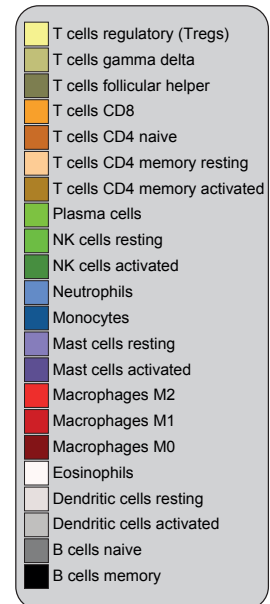
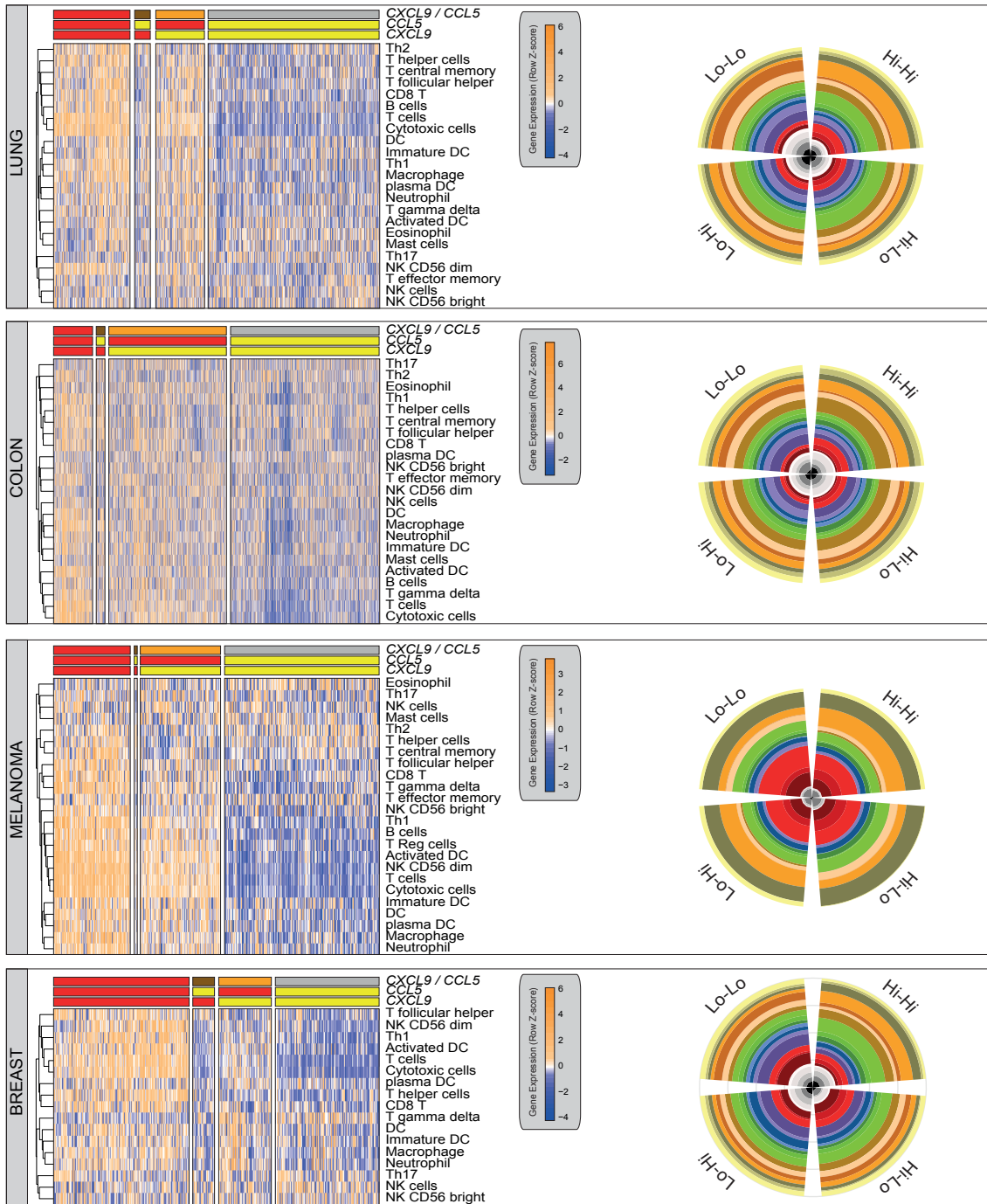
(A) *CCL5*, *CCR1*, *CCR3* and *CCR5* mRNA detection by RT-PCR in 18 ovarian cancer and normal epithelial IOSE cell lines. (B) Relative *CCL5* mRNA quantification by qPCR in FACS-sorted Epcam<sup>+</sup>CD45<sup>-</sup> ovarian cancer cells and FACS-sorted Epcam<sup>-</sup>CD45<sup>+</sup>tumor infiltrating leukocytes. Boxplots represent 25th and 75th percentiles with midline indicating the median; whiskers extend to the lowest/highest values. P value was calculated with unpaired student T test. (C) Representative FACS dot plots of CXCL9 expression in CD14<sup>+</sup> monocytes from EOC (**left**) and PBMCs (**right**). (D) Quantification of CXCL9 secretion (ELISA) of rested and IFN $\gamma$  activated monocytes, dendritic cells and T cells from healthy donors (**left**) and EOC patients (**right**). (E, F) Cytokine bead array (CBA) quantification of CXCL9 (E) and CXCL10 (F) secretion in healthy donors' blood monocytes 72 hr post stimulation with IFN $\alpha$ , IFN $\beta$  or IFN $\gamma$  (40 ng/ml). P values were calculated with multiple T tests. (G, H) Pearson correlation plots of *IFNA1* and *IFNB1* with *CXCL9* (G) or *CXCL10* (H) in ovarian cancer TCGA. R and p values are shown in each plot. (I, J) Relative quantification of IFN $\gamma$  (I) and CXCL9 (J) secretion in mixed tumor co-cultures in the presence of MHC I and/or MCH II blocking or control isotype antibodies. Shown p values were calculated with T tests comparing each condition to medium only (n=4). (K) Representative FACS dot plots of CXCR3 and CCR5 expression in autologous donor CD8<sup>+</sup> cells transduced with HLA-A\*02-restricted NY-ESO-1 TCR. All bar-graph data are presented as mean  $\pm$  SEM.

A

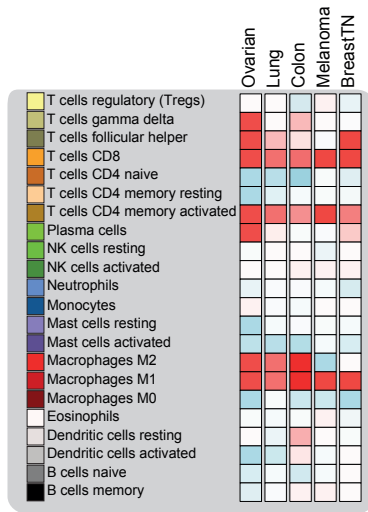
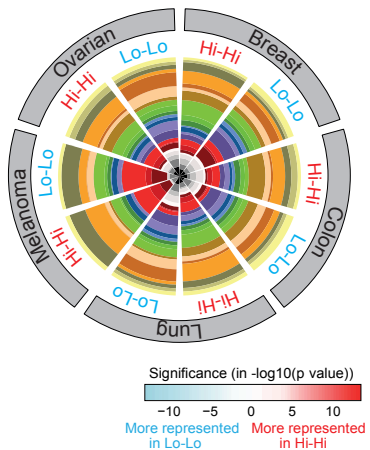
BINDEA IMMUNE SUBSETS



CIBERSORT



B



C

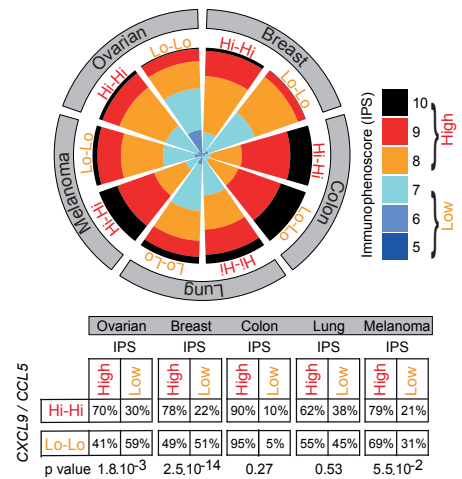


## Figure S4 related to Figure 5

### Immune landscape of triple negative breast cancer, colon cancer, lung cancer and melanoma.

(A) This figure is associated with Figure 5C and 5D and shows the equivalent panel for lung adenocarcinoma, triple-negative breast cancer, colorectal cancer and melanoma. **Left:** Heatmaps show scoring of immune gene signatures as described by Bindea et al according to *CCL5/CXCL9* chemokine expression subgroups. **Right:** Pie charts show the relative immune subset proportions computed by the CIBERSORT algorithm according to chemokine subgroups. (B) **Left:** Relative pie chart representation of immune component proportions as computed by the CIBERSORT algorithm and averaged over the *CXCL9<sup>hi</sup>CCL5<sup>hi</sup>* (Hi-Hi) and *CXCL9<sup>lo</sup>CCL5<sup>lo</sup>* (Lo-Lo) tumors from the five cancer types. **Right:** Heatmap displaying the significance level of the differences in immune subsets between Hi-Hi and Lo-Lo tumors for each cancer type (ANOVA followed by Tukey test) and the directionality of the difference (red: over-representation in Hi-Hi, light blue over-representation in Lo-Lo). (C) **Top:** Pie chart representation showing the proportion of patients with different immunophenoscores (McDonough et al.) according to their *CXCL9/CCL5* subgroups (Hi-Hi versus Lo-Lo) and cancer type. Patients were categorized into high IPS (IPS 8 to 10) and low IPS (IPS 5 to 7). **Bottom:** results of Fisher's exact tests for differences in IPS proportions between the Hi-Hi and Lo-Lo groups.

**Table S4 related to Figure 5:** Gene sets I, II and III show the genes that were common in 5, 4 and 3 cancer types, respectively.

<b>Hi-Hi genes expressed in 5/5 tumor types</b>	<b>Hi-Hi genes expressed in 4/5 tumor types</b>	<b>Hi-Hi genes expressed in 3/5 tumor types</b>
<i>CCL5</i>	<i>CIQB</i>	<i>CIQA</i>
<i>CD2</i>	<i>CCL5</i>	<i>CIQB</i>
<i>CD247</i>	<i>CD2</i>	<i>CCL5</i>
<i>CD3E</i>	<i>CD247</i>	<i>CD2</i>
<i>CD4</i>	<i>CD3D</i>	<i>CD247</i>
<i>CD53</i>	<i>CD3E</i>	<i>CD3D</i>
<i>CD86</i>	<i>CD3G</i>	<i>CD3E</i>
<i>CD8A</i>	<i>CD4</i>	<i>CD3G</i>
<i>CXCL9</i>	<i>CD53</i>	<i>CD4</i>
<i>DOCK2</i>	<i>CD86</i>	<i>CD53</i>
<i>GBP2</i>	<i>CD8A</i>	<i>CD86</i>
<i>GZMK</i>	<i>CD96</i>	<i>CD8A</i>
<i>IL10RA</i>	<i>CORO1A</i>	<i>CD96</i>
<i>IL2RB</i>	<i>CXCL9</i>	<i>CECR1</i>
<i>IRF1</i>	<i>CYBB</i>	<i>CORO1A</i>
<i>LPTM5</i>	<i>DOCK2</i>	<i>CXCL10</i>
<i>LCP1</i>	<i>EVI2B</i>	<i>CXCL9</i>
<i>PTPRC</i>	<i>GBP1</i>	<i>CYBB</i>
<i>SLC7A7</i>	<i>GBP2</i>	<i>CYTIP</i>
<i>STAT1</i>	<i>GZMA</i>	<i>DOCK2</i>
<i>TNFRSF9</i>	<i>GZMH</i>	<i>EVI2B</i>
	<i>GZMK</i>	<i>FASLG</i>
	<i>HCLS1</i>	<i>GBP1</i>
	<i>IFNG</i>	<i>GBP2</i>
	<i>IGSF6</i>	<i>GZMA</i>
	<i>IL10RA</i>	<i>GZMH</i>
	<i>IL18RAP</i>	<i>GZMK</i>
	<i>IL2RB</i>	<i>HCLS1</i>
	<i>IRF1</i>	<i>HLA.DMB</i>
	<i>ITGB2</i>	<i>HLA.DOB</i>
	<i>KLRD1</i>	<i>HLA.DPA1</i>
	<i>LAG3</i>	<i>HLA.DRA</i>
	<i>LPTM5</i>	<i>ICOS</i>
	<i>LCP1</i>	<i>IDO1</i>
	<i>LILRB4</i>	<i>IFNG</i>
	<i>MYO1F</i>	<i>IGSF6</i>
	<i>NKG7</i>	<i>IL10RA</i>
	<i>PRF1</i>	<i>IL18RAP</i>
	<i>PTPN22</i>	<i>IL2RB</i>

	<i>PTPRC</i>	<i>IRF1</i>
	<i>SH2D1A</i>	<i>ITGB2</i>
	<i>SLC7A7</i>	<i>KLRD1</i>
	<i>SRGN</i>	<i>LAG3</i>
	<i>STAT1</i>	<i>LAPTM5</i>
	<i>TNFRSF9</i>	<i>LCPI</i>
	<i>TRAF3IP3</i>	<i>LILRB4</i>
		<i>MYO1F</i>
		<i>NCKAP1L</i>
		<i>NKG7</i>
		<i>PRF1</i>
		<i>PTPN22</i>
		<i>PTPRC</i>
		<i>SH2D1A</i>
		<i>SLA</i>
		<i>SLC7A7</i>
		<i>SRGN</i>
		<i>STAT1</i>
		<i>TNFRSF9</i>
		<i>TRAF3IP3</i>
		<i>TRATI</i>

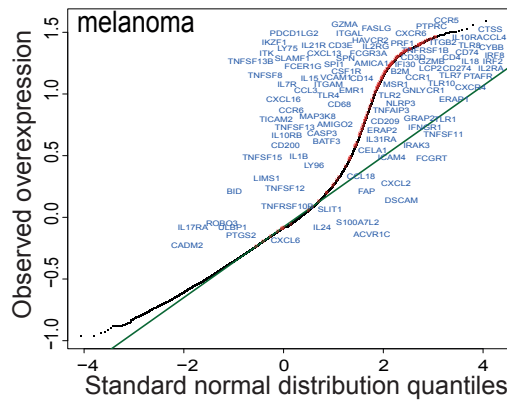
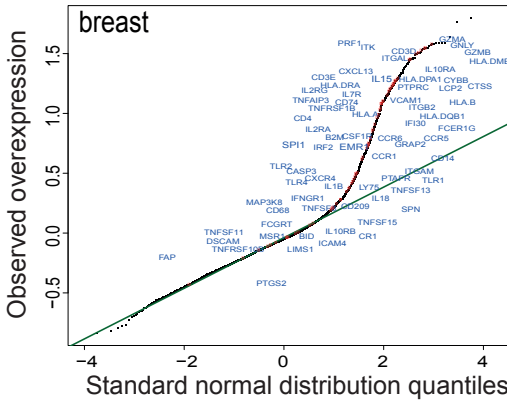
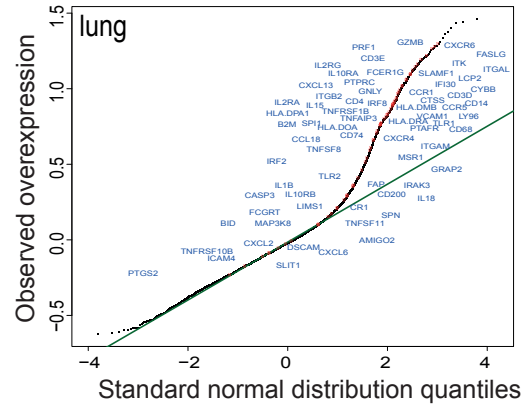
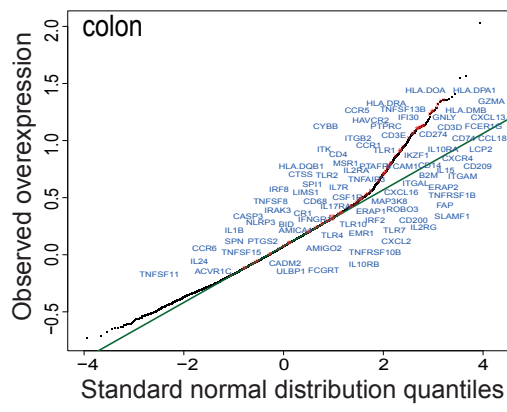
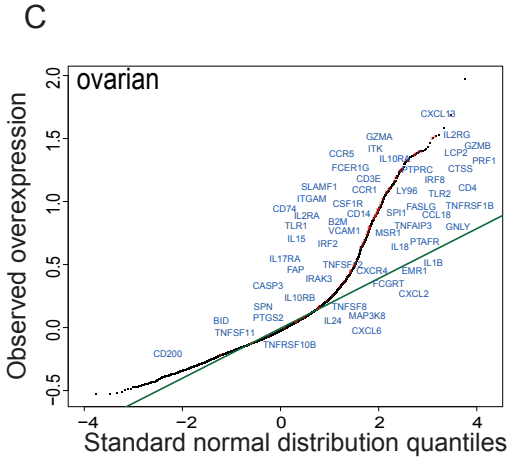
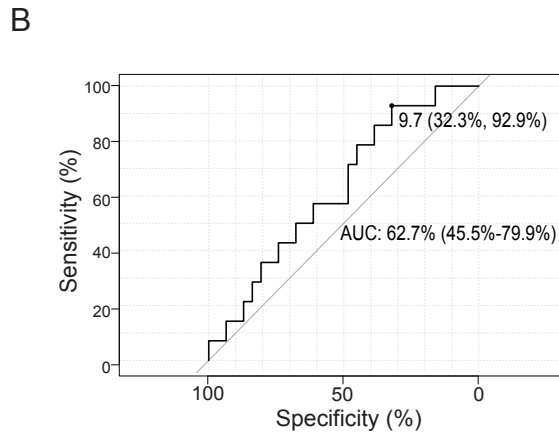
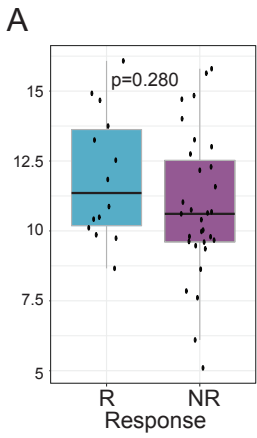


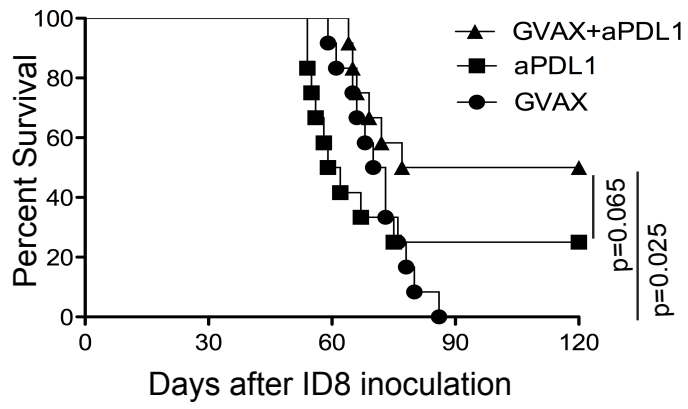
## Figure S5 related to Figure 5

### Co-expression of *CCL5* and *CXCL9* does not correlate to CTLA-4 response

(A) 21-gene chemokine signature score for pre-treatment samples are shown for responders (R) and non-responders (NR) from the the Ipilimumab-Nivolumab sequential treatment arm of Checkmate 064. Boxplots represent 25th and 75th percentiles with midline indicating the median; whiskers extend to the lowest/highest values. Points show values for individual subjects. Statistical comparison is based on one-sided Wilcoxon rank sum tests. (B) ROC plot for 21-gene signature score vs. response in the Ipilimumab-Nivolumab sequential treatment arm of Checkmate 064. (C) Position of the genes considered as upregulated under CTLA-4 and PD-1 therapy by Chen et al (Chen et al., 2016) in the Q-Q plot showing the sorted log-fold expression levels of the comparison of the Hi-Hi and Lo-Lo groups in ovarian, colon, lung, triple-negative breast cancer and melanoma. Departure from the green line Q-Q line indicates effects stronger than expected.



Early stage Treatment



Late stage Treatment

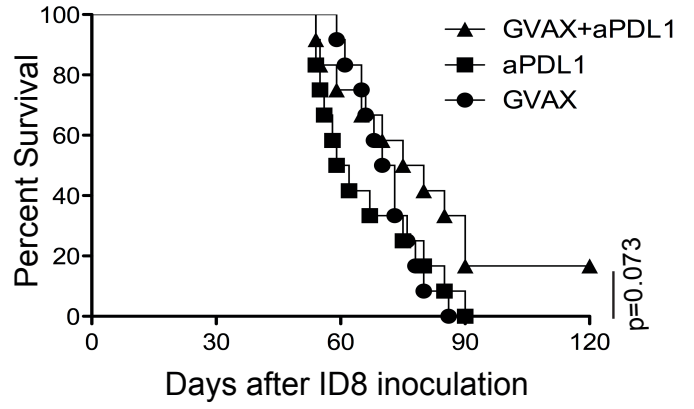


**Figure S6 related to Figure 6**

Kaplan-Meier curves showing survival of mice with intraperitoneal ID8 tumors treated at early (**left**) or late (**right**) stages with irradiated ID8-GVAX (expressing murine GM-CSF) and/or anti-PD-L1 antibody.

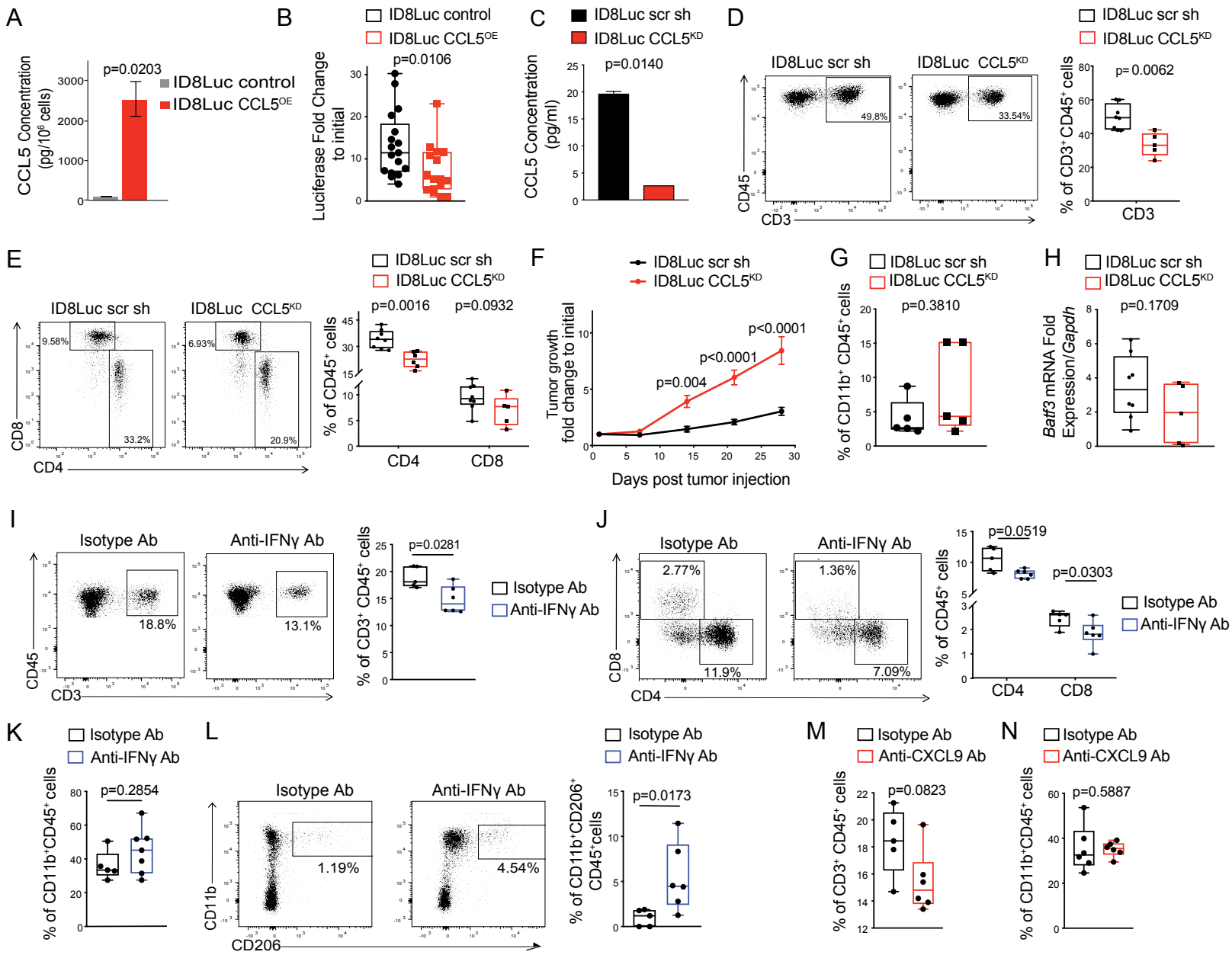


## Figure S7 related to Figure 7

### Tumor-intrinsic CCL5 defines tumor immunoreactivity and enables monocyte-derived and IFN $\gamma$ -induced CXCL9 expression *in vivo*

(A) CBA analysis of CCL5 in cell-free supernatants of ID8Luc CCL5<sup>OE</sup> and ID8Luc control cells cell lines. The concentration (pg/ml) was normalized to cell number and is represented as mean  $\pm$  SD (n=2). P value was calculated with unpaired T test. (B) Comparison of endpoint tumor growth volumes in mice injected with ID8Luc CCL5<sup>OE</sup> or ID8Luc control cells as detected bioluminescence imaging of tumor luciferase expression. P value was calculated with unpaired T test. (C) CBA analysis of CCL5 in cell-free supernatants of ID8Luc scr sh or ID8Luc CCL5<sup>KD</sup> cell lines. The concentration (pg/ml) was normalized to cell number and is represented as mean  $\pm$  SD (n=2). P value were calculated with unpaired T test. (D, E) Representative FACS dot plots and quantification of CD3<sup>+</sup> (D), CD4<sup>+</sup> and CD8<sup>+</sup> TILs (E) in ID8Luc scr sh or ID8Luc CCL5<sup>KD</sup> tumors. (F) Intraperitoneal tumor growth kinetics of ID8Luc scr sh or ID8Luc CCL5<sup>KD</sup> tumors as detected by bioluminescence imaging. Data presented as mean  $\pm$  SEM. P values were calculated with Two-way Anova T tests. (G) FACS quantification of CD11b<sup>+</sup> TAMs in ID8Luc scr sh or ID8Luc CCL5<sup>KD</sup> tumors. P value was calculated with Mann-Whitney test (H) Relative mRNA quantification of *Batf3* in ID8Luc scr sh or ID8Luc CCL5<sup>KD</sup> tumors. P value was calculated with Mann-Whitney test. (I, J) Representative FACS dot plots and quantification of CD3<sup>+</sup> (I), CD4<sup>+</sup> and CD8<sup>+</sup> (J) TILs in ID8Luc CCL5<sup>OE</sup> intraperitoneal tumors after treatment with IFN $\gamma$  blockade or isotype control antibodies. P values were calculated with Mann-Whitney test. (K) FACS quantification of CD11b<sup>+</sup> cells in the above tumors. P value was calculated with Mann-Whitney test. (L) Representative FACS dot plots and quantification of CD11b<sup>+</sup>CD206<sup>+</sup> TAMs in the above tumors. P value was calculated with Mann-Whitney test. (M, N) FACS quantification of CD3<sup>+</sup> TILs (M) and CD11b<sup>+</sup> TAMs (N) in ID8Luc CCL5<sup>OE</sup> tumors after treatment with CXCL9 neutralizing or isotype control antibodies. P values were calculated with Mann-Whitney test.

All boxplots represent 25th and 75th percentiles with midline indicating the median; whiskers extend to the lowest/highest values.